Applied Chemical Engineering (2026) Volume 9 Issue 3 ISSN: 2578-2010 (O)
doi: 10.59429/ace.v9i3.5984

RESEARCH ARTICLE

Tailoring the Morphological and Electrical Properties of PMMA-TiO2-SiC Nanocomposites for Energy Storage Applications

Rawaa Yahya Habeeb*, Majeed Ali Habeeb

University of Babylon, College of Education for Pure Sciences, Department of Physics, Iraq, Babil

***Corresponding author:** Rawaa Yahya Habeeb, Rawa.yahya1983@gmail.com

ABSTRACT

This study was conducted to develop and investigate PMMA-based nanocomposites with added nanoparticles of titanium dioxide (TiO_2) and silicon carbide (SiC). The uniqueness of this research includes combining the advantages of both TiO_2 and SiC nanoparticles for enhancing the properties of PMMA-based nanocomposites. In this study, the electrical, mechanical, and sensing performances of PMMA-TiO_2-SiC nanocomposites were examined. The fabricated nanocomposites have demonstrated significant improvements in their electrical performance, which was higher than that of pure PMMA and achieved without increasing fabrication costs or complexity. An increase in the loadings of TiO_2 and SiC nanoparticles led to an increase in the ε′, ε″, and AC electrical conductivity of the nanocomposites. The electrical conductivity of the prepared nanocomposites ranged from 3.31×10^{-11} to 1.98×10^{-10} S/cm. Measurements of the sensor response demonstrated its excellent stability in different environments, as well as superior flexibility and high-pressure sensitivity. The performance improvement can be attributed to the ability of both nanoparticles to change the structure of the material and improve charge transport. Thus, the developed multifunctional nanocomposites possess a stable electric response and could potentially be used in modern energy storage and electronic devices, such as pressure capacitive sensors.

Keywords: electrical properties, pressure sensors, dielectric loss, AC electrical conductivity

ARTICLE INFO

Received: 16 April 2026
Accepted: 22 June 2026
Available online: 31 August 2026

COPYRIGHT

Copyright © 2026 by author(s).
Applied Chemical Engineering is published by Arts and Science Press Pte. Ltd. This work is licensed under the Creative Commons Attribution-NonCommercial 4.0 International License (CC BY 4.0).
https://creativecommons.org/licenses/by/4.0/

1. Introduction

Nanoparticles possess unique structural, mechanical, optical, electrical, and magnetic properties, making nanotechnology one of the most rapidly developing and advancing scientific fields of the 21st century [1,2]. This uniqueness is primarily attributed to their extremely small dimensions, ranging from 1 to 100 nanometers, which gives them distinct physical and chemical behaviors compared to larger materials. This difference stems from the increased surface area-to-volume ratio and the emergence of size effects [3], Metal oxide nanoparticles, in particular, have garnered increasing attention due to their diverse practical applications. They are widely used in industrial catalysis, chemicals and pharmaceuticals, chemical sensors, fillers, sterilization and disinfection processes, and semiconductors, as well as being important in the cosmetics and microelectronics industries [4,5]. Polymer nanocomposites consist of a polymer matrix reinforced with nanoparticles (such as nanoparticles or nanotubes) distributed within it[6]. These materials exhibit superior performance compared to conventional polymers in terms of mechanical, thermal, and electrical properties, with the ability to modify the optical response (such as absorption, transmittance, and refractive index) depending on the type

and concentration of the filler [7-9], and they are widely employed in packaging materials and barrier films to enhance durability, reduce gas permeability, and extend product shelf life [10]. Poly(methyl methacrylate) (PMMA) is a widely used acrylic thermoplastic polymer in materials physics and polymer science applications due to its distinctive physical properties, including dimensional stability, high optical transparency, and compliance with mechanical and thermal requirements, as well as its ease of fabrication and processing. These properties have contributed to its widespread adoption in many different engineering and scientific applications[11]. Titanium dioxide nanoparticles (TiO_2) are important materials in electrical applications due to their ability to improve electrical conductivity, increase interfacial polarization, and enhance dielectric constant when incorporated into nanocomposites, making them suitable for applications in insulators, capacitors, and modern power devices. [12]. The anatase and rutile phases of titanium dioxide (TiO_2) exhibit distinct structural and functional differences that directly influence their electrical behavior. The anatase phase, with its tetragonal crystal structure, possesses a high specific surface area and a higher density of defects and surface structures, which enhances charge transport mechanisms and increases intra-material polarizability. Therefore, this phase is well-suited for applications requiring improved electrical responsiveness [13-15] Although studies on the brookite phase are limited, it exhibits similar electrical behavior and may even surpass it under certain conditions due to its different crystal arrangement. Furthermore, combining the brookite and anatase phases in a mixed structure improves the material's electrical properties by enhancing charge mobility and reducing impedance at interfaces, in addition to the synergistic effects between the different phases. This makes such mixed structures suitable for advanced electrical applications [16]. On the other hand, incorporating titanium dioxide (TiO_2) nanoparticles into a polymethyl methacrylate (PMMA) matrix significantly improves the composite's electrical properties. The nanoparticles form conductive or semiconducting pathways within the polymer matrix, enhancing charge transfer and increasing electrical conductivity. This incorporation also contributes to increased interfacial polarization due to charge accumulation at the interfaces between the nanoparticles and the polymer, leading to a higher dielectric constant and reduced losses at certain frequencies. Therefore, (PMMA–TiO_2) nanocomposites are promising materials for various electrical and electronic applications [17]. Silicon carbide (SiC) is a non-oxidizing ceramic material of wide industrial importance due to its many applications. The manufacture of silicon carbide powder began in 1893 for use in abrasive applications. Its grains can also be processed by sintering—heating the powder to a high temperature below its melting point, allowing the grains to come together and bond together, transforming it into a more cohesive, denser, and harder body without complete melting—to produce highly durable ceramic materials, justifying its use in applications requiring high precision and performance such as automotive brakes, carbide gaskets, bulletproof vests, deep drawing dies, high-speed steel polishing processes, and ceramic sheets [18]. (PMMA) polymer films doped with varying concentrations of (TiO_2) and SiC nanoparticles were fabricated using a casting method., this work aims to develop and characterize (PMMA) -based polymer nanofilms reinforced with suitable nanofillers to enhance, electrical, and mechanical properties, while also evaluating pressure sensing for flexible electronics and multifunctional materials applications.

2. Materials and Method

The nanocomposite films were prepared using solution casting, a direct and efficient technique for fabricating polymer and nanocomposite films. This method ensures a homogeneous distribution of nanoparticles within the polymer matrix, as illustrated in Figure (1). Polymethyl methacrylate (PMMA) was used as the polymer matrix with the addition of (TiO_2–SiC) in this work (PMMA) is commercially available as a white powder with a molecular weight of (430–590) kDa, according to the manufacturer (Goodfellow Cambridge Limited, UK), and an average particle size of approximately 80 μm; this value represents the polymer before dissolution and does not reflect the final structure of the formed films. (1.5) g of (PMMA) was dissolved in (35) mL of chloroform under magnetic stirring for (35min) to obtain a homogeneous solution. Subsequently, nanofillers were incorporated into the solution at different weight concentrations (2, 4, and 6

wt%) while continuing to stir to ensure uniform dispersion within the matrix. The solutions were then poured into glass Petri dishes and left to dry at room temperature for (24) hours to allow the solvent to gradually evaporate and homogeneous films to form. In the final stage, the obtained films were carefully removed from the glass dishes and collected for subsequent measurements and analyses. The thickness of the films was measured using a digital micrometer, and the measurements showed an average thickness of approximately (0.223mm) with slight variations between samples. the dielectric properties, AC current behavior, and pressure sensor response were evaluated using an LCR (3538-50 LCR Hi-TESTER, Hioki, Japan) in the [(100 – (5 × 10^6)] Hz frequency range, employing copper electrodes and measuring the equivalent capacitance as a function of the applied pressure and the evaluation of the electrical sensing efficiency of the nanocomposites.

The dielectric constant (ε') is calculated according to the following relationship [19]

$$\varepsilon_1 = \frac{C_p}{C_0} \quad (1)$$

The dielectric loss (ε'') is calculated according to the following relationship

$$\varepsilon'' = \varepsilon'. D \quad (2)$$

The AC electrical conductivity (σ_{ac}), is calculated according to the following relationship:

$$\sigma_{a.c} = \omega \varepsilon'' \varepsilon_0 \quad (3)$$

The angular frequency is represented by the symbol (ω). The sensitivity of a pressure sensor is calculated according to the following relationship [20]:

$$S_{AP}(\%) = 1 - \left(\frac{C_p}{C_n}\right) \times 100\% \quad (4)$$

When the electrical capacities of mixtures and nanocomposites with the symbols (C_p) and C_n, respectively.

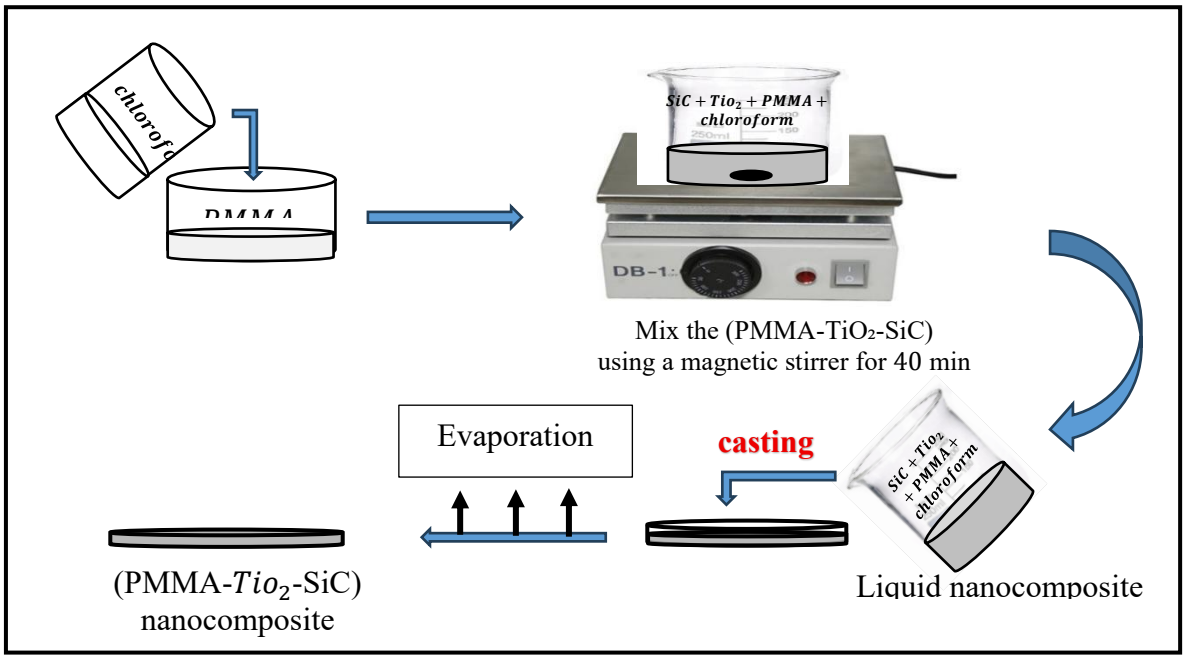


Figure 1. A diagram illustrating the steps to prepare (PMMA-TiO₂-SiC) nanocomposite.

3. Results and discussion

3.1. Optical Microscope examination of the (PMMA– TiO2 -SiC) Nanocomposite

Figure 2 shows optical microscope images of (PMMA–TiO₂-SiC) nanocomposite films at 10X magnification for samples containing (2, 4, and 6 wt.%) nanoparticles. Micrographs (A,B,C, and D) differences morphological variations directly attributable to increasing nanoparticle content within the polymer matrix.

The images demonstrate that the matrix surface structure remains cohesive, with well-integrated (TiO_2-SiC) nano particles within the film, supporting the efficiency of the preparation method. Compared to unreinforced films, gradual changes in microstructure are observed as the weight content increases from (2 wt.%) to (6 wt.%), without any significant agglomeration or noticeable deterioration in film transparency. It also appears that the highest percentage of nano-content (6 wt.%, Figure D) gives the best regularity and spread of particles within the matrix, which is consistent with previous reports [21,22].

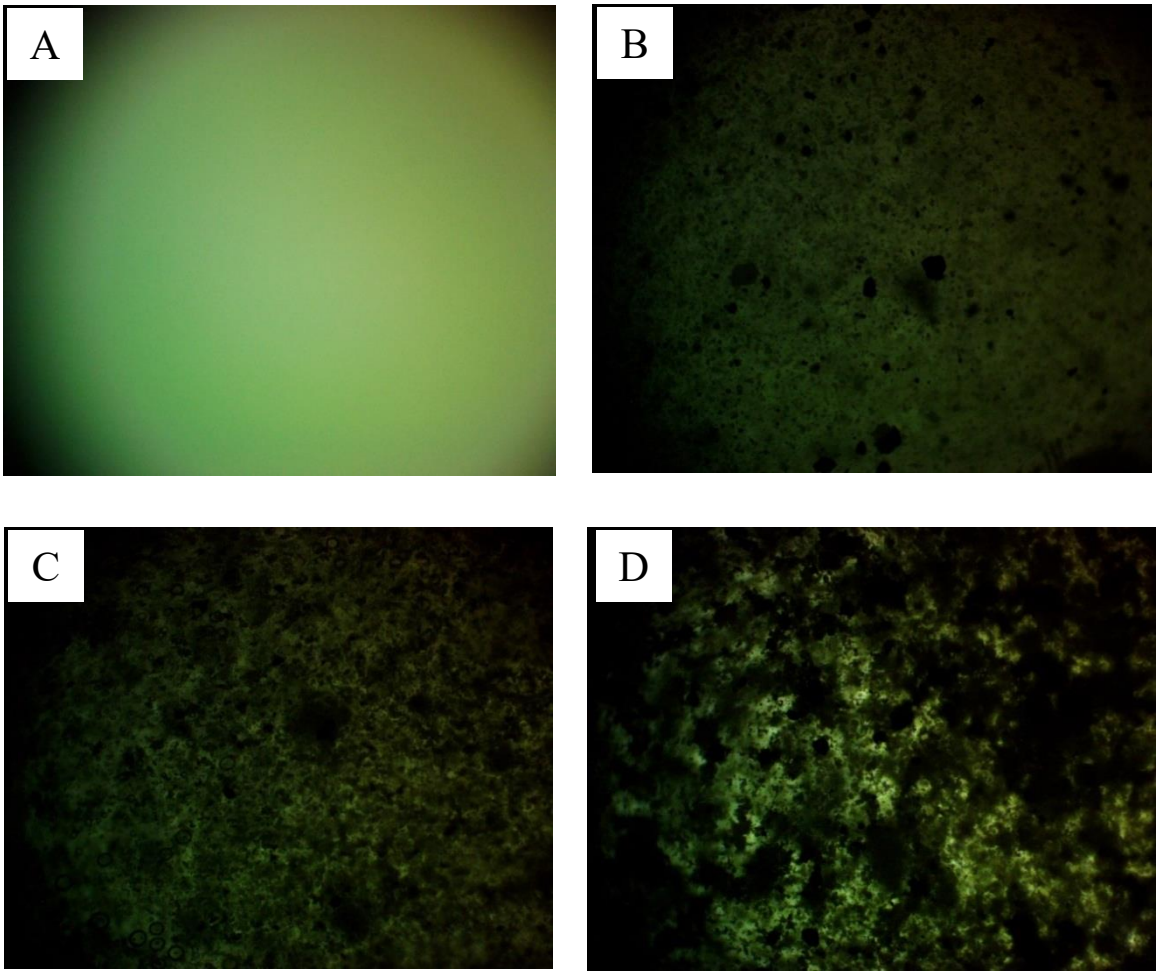


Figure 2. Optical microscope images (10X) for (PMMA-TiO_2-SiC) Nanocomposite: A (pure), B (2 wt.% of TiO_2-SiC), C (4 wt.% of TiO_2-SiC), D (6 wt.% of TiO_2-SiC).

3.2. The A.C Electrical Properties of (PMMA–TiO2-SiC) nanocomposites

Figure 3 shows the change in the dielectric constant (Ɛ′) with frequency (10^2–10^6 Hz) for pure polymer samples and nanocomposites containing (TiO_2) at percentages of (2,4,6 wt.%). It is observed that (Ɛ') decreases with increasing frequency in all samples. This can be explained by the fact that the dipoles and internal orientations in the material are able to respond to the field at low frequencies, but as the frequency increases, the field changes faster than their ability to follow, thus reducing their contribution to the overall polarization and decreasing the dielectric constant. The results also show that the addition of (TiO_2) increases the values of (Ɛ') compared to the pure sample, and the values increase with increasing weight percentage, indicating an improvement in the material's polarizability with increasing nanoparticle content [23]. As seen in Table 1.

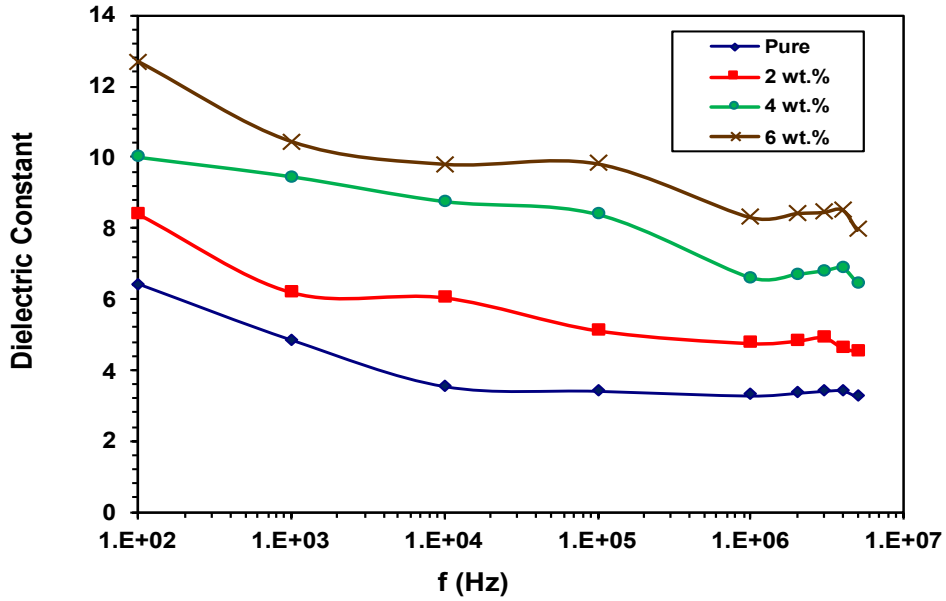


Figure 3. Change in dielectric constant with frequency for (PMMA–TiO_2-SiC) nanocomposites.

Figure 4 illustrates the change in dielectric loss (ε") with frequency for (PMMA–TiO_2-SiC) nanocomposites. The figure shows that the (ε") valuesare high at low frequencies and then gradually decrease with increasing frequency in all samples. This can be explained by the fact that the response within the material is more pronounced at low frequencies because the movable internal components can follow changes in the electric field, resulting in higher energy loss. At higher frequencies, the field changes become faster, and this response cannot follow as efficiently, thus reducing the dielectric loss. It is also observed that increasing the nanoparticle content generally leads to higher (ε") values compared to the pure sample, reflecting the increased contribution of the nanoparticles within the matrix. At the end of the high frequency range, a slight rise in some curves is observed, which can be attributed to conductivity effects at high frequencies within the measurement range [24,25]. As seen in Table 1.

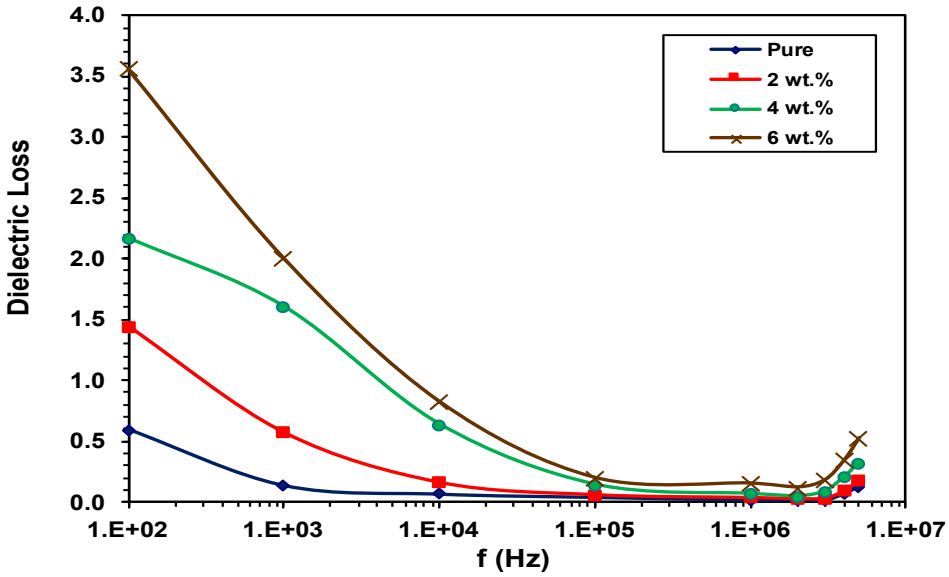


Figure 4. Change in dielectric loss with frequency for (PMMA–TiO_2-SiC) nanocomposites.

Figure 5 shows that the alternating electrical conductivity (σ_{ac}) increases with increasing frequency for all samples, and its values rise significantly with increasing (TiO_2-SiC) content, reaching their highest point at (6%), followed by (4%) and (2%), compared to the pure sample. This behavior is attributed to improved charge transport within the compound at higher frequencies. Additionally, the presence of nanoparticles contributes to enhancing the conduction pathways within the polymer matrix, leading to an increase in (σ_{ac}) [26,27].

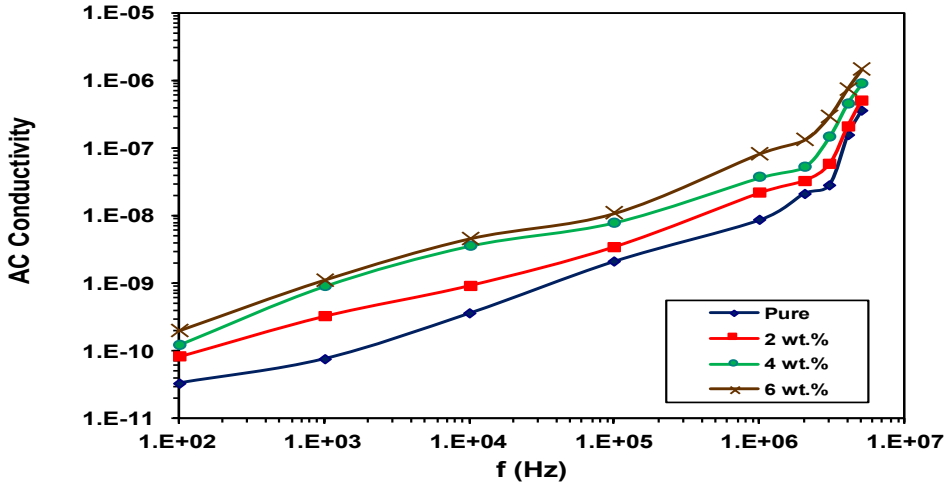


Figure 5. Variation of AC electrical conductivity as a function of frequency for (PMMA–TiO_2-SiC) nanocomposites.

Table 1. Values of dielectric constant (Ɛ′), dielectric loss ε"), and (AC) electrical conductivity σ_{ac} of (PMMA-TiO_2–SiC) nanocomposites.

Con of TiO_2/SiC wt.%	Ɛ′	ε"	$\sigma_{a.c}$ (S/cm)
0	6.402	0.595	3.31×10^{-11}
2	8.387	1.442	8.02×10^{-11}
4	9.996	2.169	1.21×10^{-10}
6	12.670	3.560	1.98×10^{-10}

Figure (6) illustrates the effect of (TiO_2-SiC) nanoparticle concentration on the behavior of the real part of the dielectric constant (ε′) of (PMMA) composites at different frequencies. The results show that the value of (ε′) gradually increases with increasing (TiO_2-SiC) content. This is attributed to the enhanced polarization within the polymer matrix at higher concentrations, particularly due to the aggregation of nanoparticles within the nanocomposite, which increases the material's ability to store electrical energy [28].

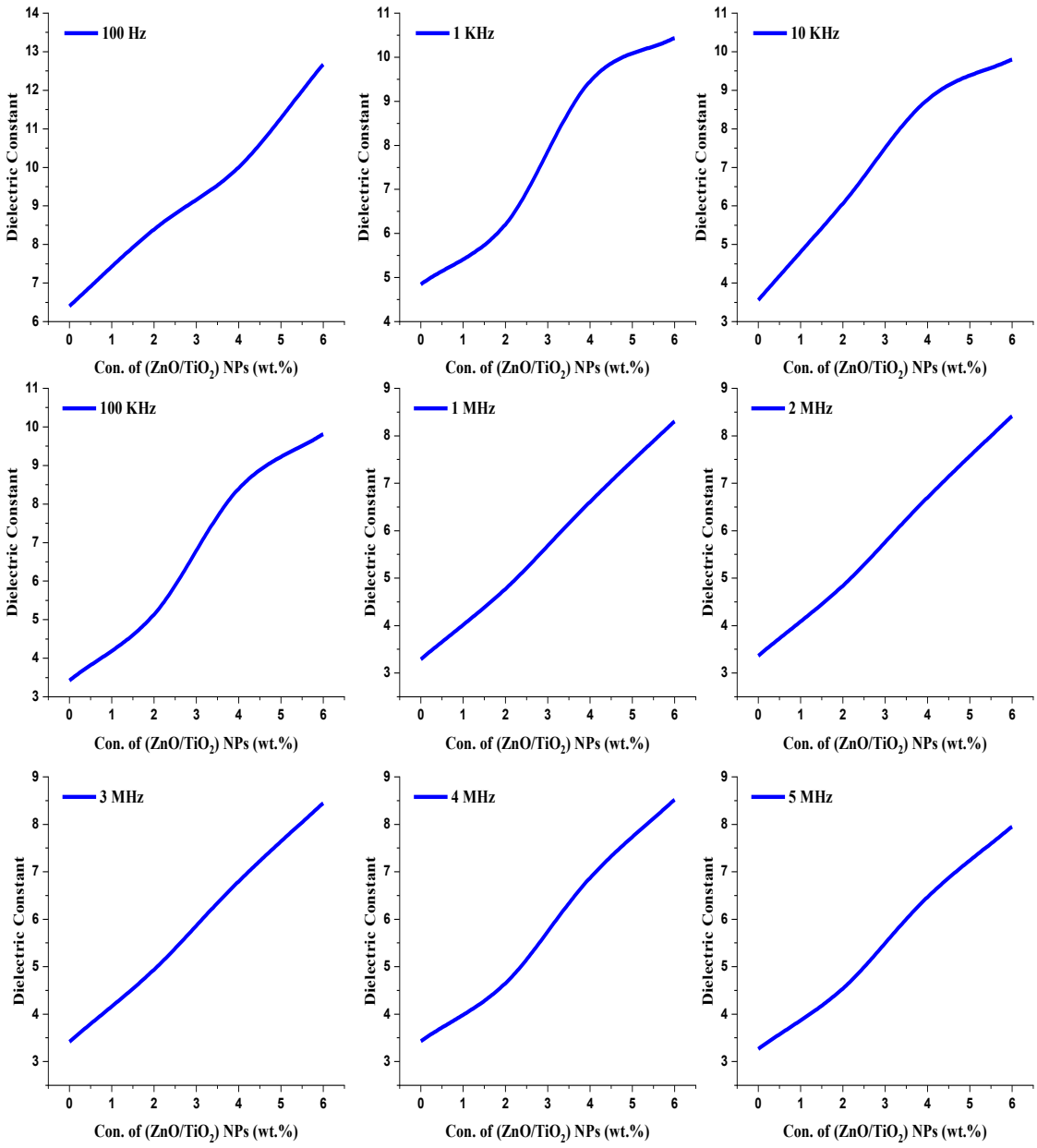


Figure 6. Dielectric constant (ε′) of (PMMA) polymer with (TiO_2-SiC) nanoparticles concentration at different frequencies.

Figure (7) shows that the dielectric loss (ε″) increases with increasing proportion of (TiO_2 -SiC) particles within (PMMA) at different frequencies. At low frequencies, the charges have sufficient time to move and accumulate at the interfaces between the polymer and the nanoparticles, resulting in a greater loss. At high frequencies, the direction of the magnetic field changes rapidly, and the charges cannot fully keep pace, thus reduce their responsiveness and weaken their effect compared to lower frequencies. In general, increasing the nanoparticle content increases the number of charges and contact areas within the composite, which raises the value of (ε″) due to increased energy dissipation within the material [29].

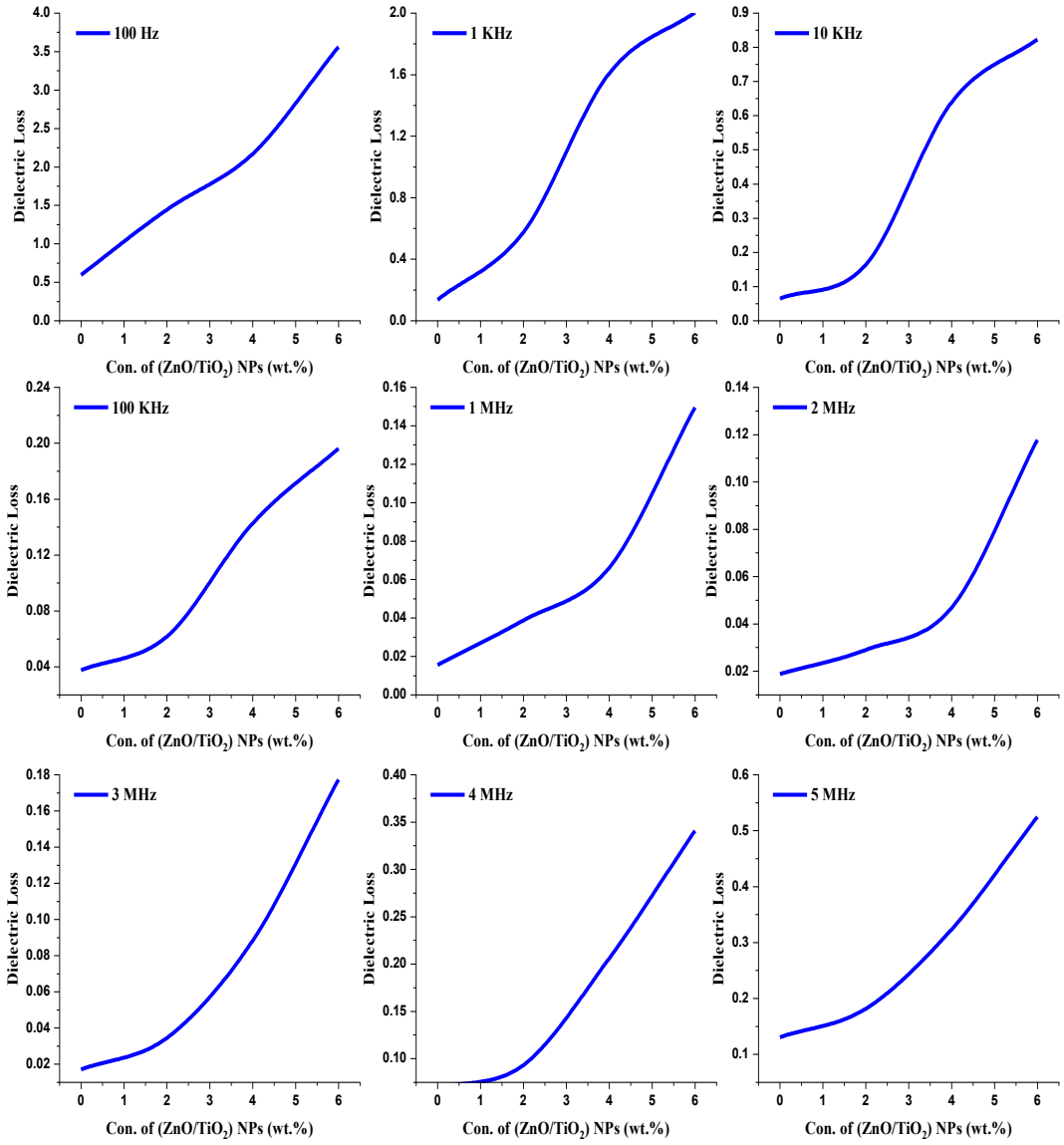


Figure 7. Dielectric loss (ε″) of (PMMA) polymer with (TiO_2-SiC) nanoparticles concentration at different frequencies.

Figure 8 illustrates the alternating electrical conductivity (σ_{ac}) of (PMMA) nanocomposites reinforced with (TiO_2-SiC) nanoparticles over a frequency range of (1×10^2 to 5×10^6) Hz. The results show that (σ_{ac}) increases with frequency and with increasing nanoparticle concentration. At low frequencies, charge transport is relatively limited due to the accumulation of charge carriers at the interfacial regions within the composite. However, increasing the frequency enhances the carrier response to the alternating field and facilitates their movement between sites, thus increasing the conductivity. Furthermore, increasing the (TiO_2-SiC) content increases the carrier density and enhances conduction pathways within the matrix, which explains the observed increase in (σ_{ac}) [30].

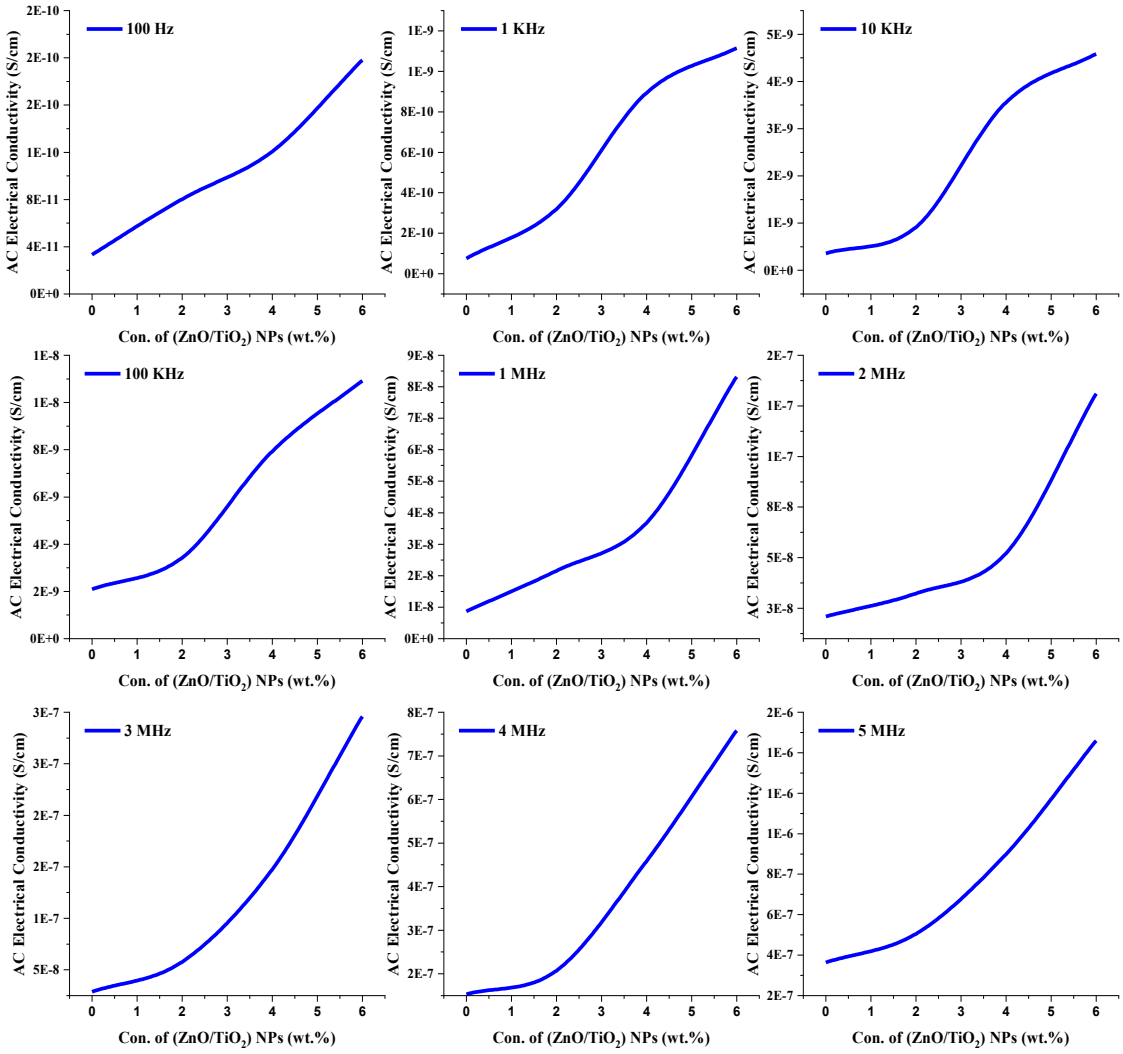


Figure 8. Illustrates effect of (TiO_2-SiC) nanoparticles on the electrical conductivity of (PMMA) at different frequencies.

3.3. Application of (PMMA–TiO2-SiC) Nanocomposites for Pressure Sensors

Figure 9 the parallel capacitance behavior of (PMMA-TiO_2-SiC) nanocomposites under varying pressures and at different weight percentages of nanoparticles (Pure, 2wt.%, 4wt.%, 6 wt.%). The figure shows a clear direct relationship between the parallel capacitance and the applied pressure for all samples; the capacitance values increase with increasing pressure, and the capacitance increases even more with increasing nanoparticle filler percentage. The (6wt.%) sample exhibits the highest values compared to the other samples within the studied pressure range. This behavior can be explained by the fact that applying pressure leads to a rearrangement of the polarization within the nanocomposite's physical structure. In the mechanically unloaded state, the dipole moments are distributed in a quasi-random manner, thus reducing the overall polarization. With increasing mechanical stress, the local distribution of dipole moments changes and their alignment increases, which enhances polarization and contributes to an increase in the charge stored at the interfaces, thus increasing the parallel capacitance. Furthermore, the presence of nanoparticles at higher concentrations enhances the density of effective polarization centers and strengthens the effect of the local field within the material, resulting in a more pronounced capacitive response to pressure [30].

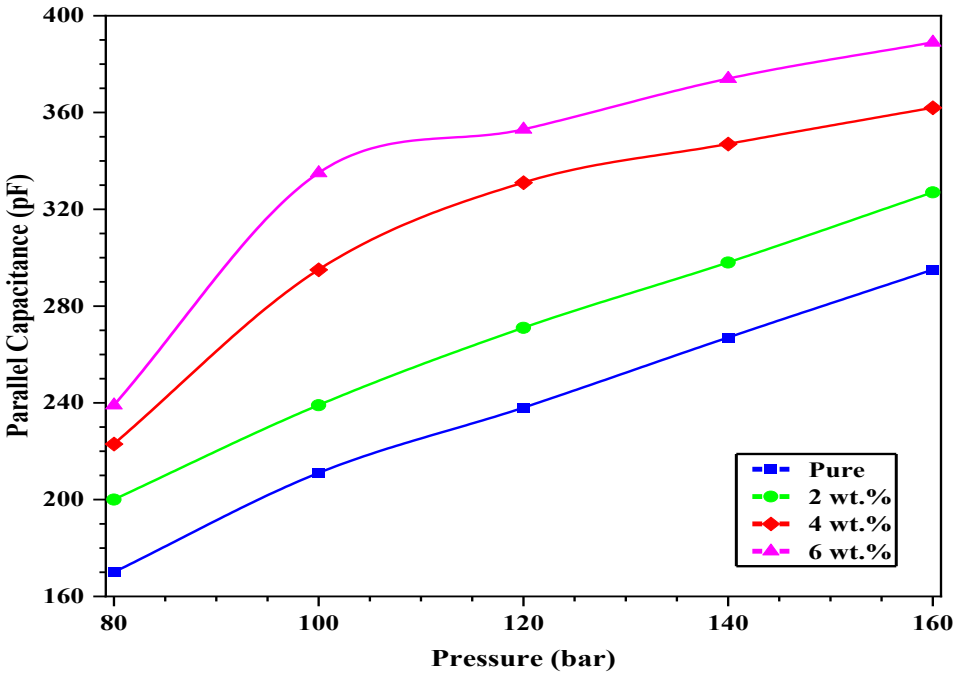


Figure 9. Parallel capacitance versus pressure for (PMMA–TiO_2-SiC) nanocomposites.

Figure 10 illustrates the change in parallel capacitance (C_p) of (PMMA-TiO_2-SiC) nanocomposites with pressure (0–6 bar) for samples with different weight percentages of nanofiller (pure, 2wt.%, 4wt.%, and 6wt.%). The figure shows a direct relationship between pressure and capacitance values for all samples, with (C_p) gradually increasing as pressure increases. The results also show that increasing the nanoparticle percentage leads to an increase in capacitance at each pressure value; the (6wt.%) sample exhibits the highest values, followed by the (4wt.%) sample, then the (2wt.%) sample, and finally the pure sample. Furthermore, the increase is most pronounced at low pressures (up to approximately 2 bar), and the curves tend to show a slower growth rate at higher pressures, indicating that the response is approaching near-saturation. This behavior is attributed to the fact that the introduction of (TiO_2-SiC) particles enhances polarization and charge accumulation at the interfaces (interfacial polarization) and improves charge transport pathways within the polymer matrix, resulting in increased capacitance under mechanical load [31].This response is important for pressure sensor applications because the sensitivity of the sensing element and the extent of (C_p) change depend directly on the content and distribution of the nanofiller within the active layer [31].

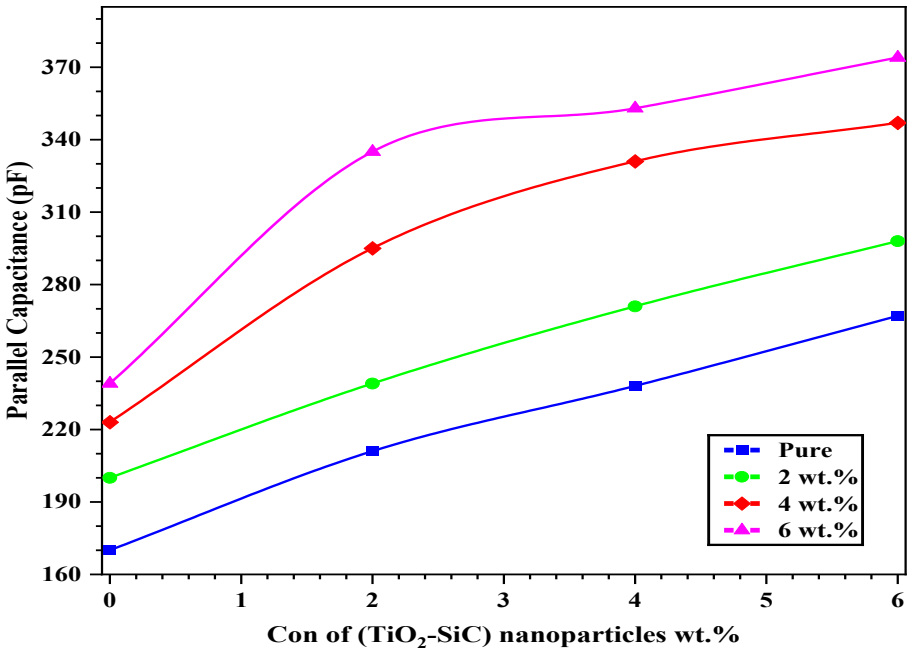


Figure 10. Parallel capacitance (C_p) dependence on pressure in (PMMA–TiO_2-SiC) nanocomposites.

Figure 11 illustrates the effect of (TiO_2-SiC) nanoparticle concentration on the sensitivity of (PMMA) polymer pressure sensors. The results show that sensitivity gradually increases with increasing nanoparticle content from (0 to 6) wt%, with no decrease observed at lower concentrations. This behavior is attributed to enhanced interfacial polarization mechanisms within the polymer matrix and increased interactions at the interfaces between the nanoparticles and (PMMA), leading to improved sensor response to pressure and higher sensitivity at higher concentrations [32].

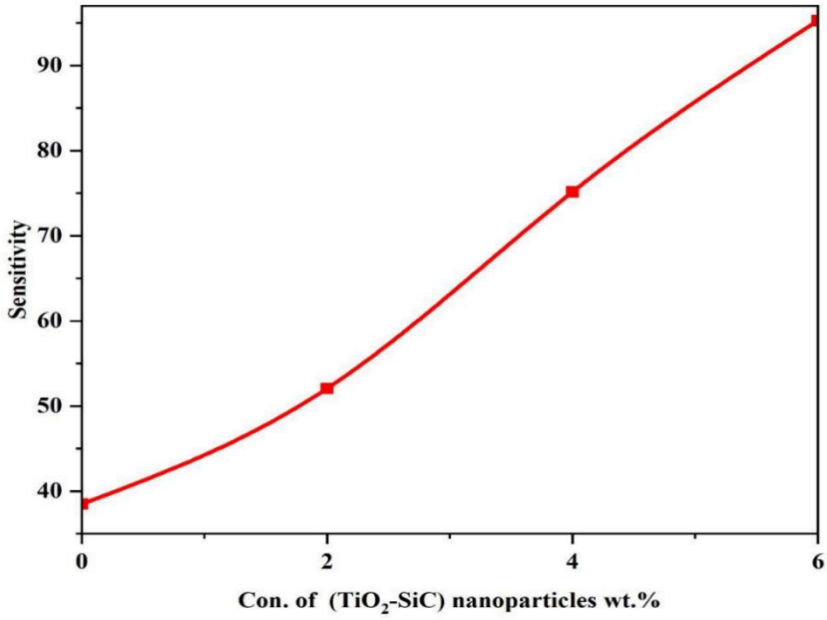


Figure 11. Pressure sensor sensitivity based on (PMMA) polymer as a function of (TiO_2-SiC) nanoparticle concentration.

4. Conclusion

Indeed, as the current study has shown, the introduction of TiO_2–SiC nanoparticles to PMMA results in an improvement of the electrical properties of the developed nanocomposites. Namely, the dielectric constant and dielectric loss as well as AC conductivity have been found to grow as the amount of nanoparticles added grows. It is believed that this effect can be accounted for by improved interface polarization, enhanced charge mobility and polymer-nanoparticle interaction. Speaking of the practical applications, it should be noted that the obtained PMMA–TiO_2–SiC nanocomposites possess stable and highly sensitive performance as capacitive pressure sensors upon mechanical load. In general, the developed PMMA-based nanocomposites with TiO_2–SiC nanoparticles appear to provide more pronounced electrical and functional effects compared to pure PMMA and outperform other conventional materials considered previously.

References

1. N. N. Shabah, T. T. K. Rahman, R. Gopika, and M. T. Ramesan, "Multifunctional polyvinyl alcohol / maranta arundinacea starch /LiAgO nanocomposites: A sustainable approach for antibacterial and optoelectronic applications," Journal of Thermoplastic Composite Materials, Jul. 2025, doi: 10.1177/08927057251359540.
2. E. Džunuzović, K. Jeremić, and J. M. Nedeljković, "In situ radical polymerization of methyl methacrylate in a solution of surface modified TiO2 and nanoparticles," Eur. Polym. J., vol. 43, no. 9, pp. 3719–3726, Sep. 2007, doi: 10.1016/j.eurpolymj.2007.06.026.
3. Z. K. Heiba, A. Badawi, E. E. Ali, R. M. Ibrahim, and M. B. Mohamed, "Controlling the Radiation Shielding and Fluorescence Features of Polyvinyl Alcohol/Polyvinyl Pyrrolidone/Polyethylene Glycol by Incorporation with Erbium Doped Cobalt Ferrite Nanofillers," Journal of Macromolecular Science, Part B, vol. 64, no. 7, pp. 763–784, Jul. 2025, doi: 10.1080/00222348.2025.2470506.
4. K. S. Hemalatha, K. Rukmani, N. Suriyamurthy, and B. M. Nagabhushana, "Synthesis, characterization and optical properties of hybrid PVA–ZnO nanocomposite: A composition dependent study," Mater. Res. Bull., vol. 51, pp. 438–446, Mar. 2014, doi: 10.1016/j.materresbull.2013.12.055.
5. W. K. Kadhim, M. A. Habeeb, Fabrication and Tuning the Morphological, Structural and Dielectric Characteristics of PVA-PEG-SiO_2-Co_2O_3 Nanocomposite Films for Nanoelectronics and Energy Storage Devices, Silicon, 16(10), pp. 4241–4251, 2024, https://doi.org/10.1007/s12633-024-02998-7
6. A. M. El-naggar et al., "Embedding of 50%PVA/50%PVP blend with Sn0.75M0.25S2, (M = Y, Fe, Cr, V); structural and optical study," Applied Physics A, vol. 127, no. 10, p. 753, Oct. 2021, doi: 10.1007/s00339-021-04905-y.
7. A. A. Mohammed, N. K. Al-Sharifi, M. A. Habeeb, Fabrication and exploring the structural, dielectric and optical features of PVA/SnO_2/Cr_2O_3 nanostructures for optoelectronic applications, Optical and Quantum Electronics, Vol.55 , Issu. 11: 1016 (2023), https://doi.org/10.1007/s11082-023-05261-2
8. A. J. Kalladi and M. T. Ramesan, "Green-Synthesized Zinc Oxide/Polyvinyl Alcohol /Cashew Gum/Polypyrrole Nanocomposites With Enhanced Mechanical, Thermal, and Electrical Properties for Nanoelectronics," J. Appl. Polym. Sci., vol. 142, no. 14, Apr. 2025, doi: 10.1002/app.56686.
9. A. M. El Nahrawy, B. A. Hemdan, A. M. Mansour, A. Elzwawy, and A. B. Abou Hammad, "Integrated use of nickel cobalt aluminoferrite/Ni2+ nano-crystallites supported with SiO2 for optomagnetic and biomedical applications," Materials Science and Engineering: B, vol. 274, p. 115491, Dec. 2021, doi: 10.1016/j.mseb.2021.115491.
10. A. M. El Nahrawy, B. A. Hemdan, A. B. Abou Hammad, A. M. Othman, A. M. Abouelnaga, and A. M. Mansour, "Modern Template Design and Biological Evaluation of Cephradine-loaded Magnesium Calcium Silicate Nanocomposites as an Inhibitor for Nosocomial Bacteria in Biomedical Applications," Silicon, vol. 13, no. 9, pp. 2979–2991, Sep. 2021, doi: 10.1007/s12633-020-00642-8.
11. D. AGOP-FORNA, P. S. POPA, and G. V. POPA, "PMMA IN DENTISTRY: A MODERN SOLUTION FOR SUSTAINABLE DENTAL RESTORATIONS," Medicine and Materials, vol. 4, no. 2, pp. 77–84, Jun. 2024, doi: 10.36868/MEDMATER.2024.04.02.077.
12. R.S. Abdul Hamza, M. A. Habeeb , Structural and Dielectric Parameters of PVA/CMC Blend Reinforced with SiO_2/SnO_2 Nanoparticles for Nanoelectronics Applications, Transactions on Electrical and Electronic Materials, 25(1), pp. 77–88,2024, https://doi.org/10.1007/s42341-023-00486-0
13. A. N. El-Shazly, A. H. Hegazy, M. M. Rashad, M. F. El-Shahat, and N. K. Allam, "Ultrathin ALD TiO2 shells for enhanced photoelectrochemical solar fuel generation," J. Alloys Compd., vol. 739, pp. 178–183, Mar. 2018, doi: 10.1016/j.jallcom.2017.12.218.
14. M. J. Gázquez, S. M. P. Moreno, and J. P. Bolívar, "TiO2 as white pigment and valorization of the waste coming from its production," in Titanium Dioxide (Tio₂) and Its Applications, Elsevier, 2021, pp. 311–335. doi: 10.1016/B978-0-12-819960-2.00011-0.

15. R. Kaplan, B. Erjavec, G. Dražić, J. Grdadolnik, and A. Pintar, “Simple synthesis of anatase/rutile/brookite TiO2 nanocomposite with superior mineralization potential for photocatalytic degradation of water pollutants,” Appl. Catal. B, vol. 181, pp. 465–474, Feb. 2016, doi: 10.1016/j.apcatb.2015.08.027.
16. R. B. Rajput and R. B. Kale, “Photocatalytic activity of solvothermally synthesized rutile TiO2 nanorods for the removal of water contaminants,” Materials Science and Engineering: B, vol. 294, p. 116556, Aug. 2023, doi: 10.1016/j.mseb.2023.116556.
17. N. K. Al-Sharifi, A. A. Mohammed, I. Oreibi, M.A. Habeeb, R. S. Abdul Hamza, Synthesized Polymeric Nanocomposites with Enhanced Optical and Electrical Characteristics Based on SiO_2 Nanoparticles for Multifunctional Technological Applications, Journal of Electronic Materials, 53 (10), pp. 6498–6507, 2024, https://doi.org/10.1007/s11664-024-11298-0
18. Z. Yan, J. Zhao, R. Liu, B. Liu, Y. Shao, and M. Liu, “An insight into sintering mechanisms of silicon carbide nanoparticles with additives using MD simulation,” Powder Technol., vol. 431, p. 119053, Jan. 2024, doi: 10.1016/j.powtec.2023.119053.
19. M. H. Abdel-Kader, M. B. Mohamed, T. Alharby, and R. M. Ibrahim, “UV-Irradiation Effects on the Structural, Optical and Electrical Characteristics of Soft Blended Polymeric Materials Loaded with Multi-Walled Carbon Nanotubes (MWCNTs),” Journal of Macromolecular Science, Part B, vol. 64, no. 5, pp. 531–554, May 2025, doi: 10.1080/00222348.2024.2357916.
20. S. M. A. Zaidi, M. A. Kalyar, Z. A. Raza, A. Shoukat, R. Waseem, and M. Aslam, “Effect of laser irradiance on opto-electrical properties of PVA embedded graphene copper ferrite nanocomposite strips,” Opt. Mater. (Amst)., vol. 147, p. 114590, Jan. 2024, doi: 10.1016/j.optmat.2023.114590.
21. R.S. Abdul Hamza, M. A. Habeeb , Fabrication and Exploring the Morphological, Structural and Optical Characteristics of Polyvinyl Alchol—Carboxymethyl Cellulose—Silicon Dioxide—Tin Dioxide Nanostructures for Optoelectronics and Antibacterial Applications, Silicon, 16 (3), pp. 1043–1056, 2024, https://doi.org/10.1007/s12633-023-02735-6
22. W. M. Almalki et al., “Enhanced dielectric, optical, and electrical conductivity in polymer nanocomposites films via loading LiCl/ZnO nanoparticles for energy storage and organic optoelectronic devices,” Macromol. Res., vol. 33, no. 10, pp. 1337–1347, Oct. 2025, doi: 10.1007/s13233-025-00419-1.
23. I. Oreibi, M. A. Habeeb, R.S. Abdul Hamza, F. Mamoun, Synthesis and Tuning the Morphological, Structural, Optical and Dielectric Features of SiO2/CuO Futuristic Nanocomposites Doped PVA–PEG for Optoelectronic and Energy Storage Applications, Journal of Inorganic and Organometallic Polymers and Materials, Vol. 35. No. 4, pp. 2391-2405, 2025, https://doi.org/10.1007/s10904-024-03334-7
24. L. Zhang, S. Zhang, C. Wang, Q. Zhou, H. Zhang, and G.-B. Pan, “Highly Sensitive Capacitive Flexible Pressure Sensor Based on a High-Permittivity MXene Nanocomposite and 3D Network Electrode for Wearable Electronics,” ACS Sens., vol. 6, no. 7, pp. 2630–2641, Jul. 2021, doi: 10.1021/acssensors.1c00484.
25. A. Rajeh et al., ‘Alteration in the Structural, Optical, Thermal, Electrical, and Dielectric Properties of PMMA/PVDF Blend by Incorporation of Ni/ZnO Nanohybrid for Optoelectronic and Energy Storage Devices’, J Inorg Organomet Polym Mater, vol. 34, no. 3, pp. 1221–1231, Mar. 2024, doi: 10.1007/s10904-023-02880-w.
26. R. S. Abdul Hamza and M. A. Habeeb, “Synthesis, Characterization and Application of PVA– CMC/SiO2–Cr2O3 Nanostructures,” Nanosistemi, Nanomateriali, Nanotehnologii, vol. 22, no. 1, pp. 107–118, 2024, doi: 10.15407/nnn.22.01.107.
27. Z. K. Heiba, S. A. Mouhammad, A. Badawi, and M. B. Mohamed, “Integrating the Structural, Dielectric, and Radiation Shielding Features of ZnO/Co Nanoparticles Filled PVA/PVP/PEG Blend for Energy Storage and Radiation Shielding Applications,” ECS Journal of Solid State Science and Technology, vol. 14, no. 5, p. 053007, May 2025, doi: 10.1149/2162-8777/add6d8.
28. A. M. El-naggar, Z. K. Heiba, A. M. Kamal, and M. B. Mohamed, “Enhanced Optical and Dielectric Characteristics of PVC/PEG Blended Polymer via Loading $ZnCo_{1.8}Al_{0.2}O_4$ /LiTFSI/THAI for Emerging Optical and Electrical Applications,” ECS Journal of Solid State Science and Technology, vol. 14, no. 1, p. 013010, Jan. 2025, doi: 10.1149/2162-8777/adac8e.
29. J. Satheesh Goud and N. Narsimlu, “Synthesis and characterization of Fe2O3 nanoparticles incorporated PVA nanocompositefilms,” Indian Journal of Chemical Technology, vol. 29, no. 6, pp. 737–744, Nov. 2022, doi: 10.56042/ijct.v29i6.
30. L. A. M. Al-Sagheer and A. Rajeh, “Synthesis, characterization, electrical, and magnetic properties of polyvinyl alcohol/carboxymethyl cellulose blend doped with nickel ferrites nanoparticles for magneto-electronic devices,” Polym. Compos., vol. 44, no. 10, pp. 7156–7169, Oct. 2023, doi: 10.1002/pc.27624.
31. M. Shahmohammadi, B. E. Nagay, V. A. R. Barão, C. Sukotjo, G. Jursich, and C. G. Takoudis, “Atomic layer deposition of TiO2, ZrO2 and TiO2/ZrO2 mixed oxide nanofilms on PMMA for enhanced biomaterial functionalization,” Appl. Surf. Sci., vol. 578, p. 151891, Mar. 2022, doi: 10.1016/j.apsusc.2021.151891.
32. S. I. Qashou, E. F. M. El-Zaidia, A. A. A. Darwish, and T. A. Hanafy, “Methylsilicon phthalocyanine hydroxide doped PVA films for optoelectronic applications: FTIR spectroscopy, electrical conductivity, linear and nonlinear optical studies,” Physica B Condens. Matter, vol. 571, pp. 93–100, Oct. 2019, doi: 10.1016/j.physb.2019.06.063.